Online ISSN: 2981-0396 Print ISSN: 2981-0388

International Journal of Iron & Steel Society of Iran

Journal Homepage: https://journal.issiran.com/

Research Article

Characterization of a Novel Zr-based Thin Film Metallic Glass Applied on 316 Stainless Steel Substrate

H. Shafyei [1], A. Seifoddini *[2], S. Hasani [3], A. Obeydavi [4]

[1,2,3] Department of Mining and Metallurgical Engineering, Yazd University, Yazd, Iran
[4] Department of Materials Engineering, Isfahan University of Technology, Isfahan, Iran

ARTICLE INFO

Keywords:

316 stainless steel, Zr-based TFMG, Antibacterial properties, Roughness, Surface free energy, Contact angle, Corrosion behavior.

Article history:

Received 29 July 2024
Received in revised form 03 August 2024
Accepted 11 August 2024

ABSTRACT

316 stainless steel is one of the alloys commonly used for surgical instruments. When in contact with bacteria, these tools are highly prone to contamination. By applying coatings with high antibacterial properties, this problem can be significantly mitigated. This research aims to design a novel Zr-based alloy with a glass structure based on Zr that has antibacterial properties and is applied to 316 stainless steel. First, an alloy with the chemical composition $Zr_{30}Cu_{20}Al_{10}Ag_{10}Cr_{10}Si_{10}B_{10}$ was designed and produced. Next, thin alloy layers were deposited on 316 steel samples using a DC Magnetron Sputtering machine. The GIXRD tests indicated success in obtaining a completely amorphous structure. The antibacterial behavior of the created coating against two bacteria, Escherichia coli and Staphylococcus aureus, was investigated. The results showed that the coating exhibited high antibacterial properties against these bacteria. Additionally, applying the new coating can play an essential role in the adhesion of various cancer cells to surgical tools made from 316 stainless steel due to the reduction of substrate roughness by approximately 50%. Tests showed that the application of the designed coating reduced the energy of the surface, increased the contact angle, and thus increased the hydrophobicity of the surface, transforming the surface of 316 stainless steel from hydrophilic to hydrophobic. Furthermore, the amorphous coating structure enhanced the corrosion resistance of the 316 steel in 3.5% NaCl solution. Therefore, applying the newly designed coating to biomedical steel tools is suggested.

1. Introduction

316 stainless steel is widely used to manufacture medical equipment, including surgical tools. These tools become highly contaminated when they come into contact bacteria [1]. For this reason, applying coatings with antimicrobial or non-sticking properties on the surfaces of these instruments is a significant research subject. Studies show that one of the newest coatings attracting researchers' attention as antibacterial coatings is Zr-based coatings with an amorphous structure.

The presence of copper, silver, or aluminum in these coatings imparts antimicrobial properties [2-6]. Consequently, the US Environmental Protection Agency has registered copper as the first solid antimicrobial substance. Silver ions, when adhering to bacteria, can easily enter bacterial cells, block their respiratory systems, and destroy their energy production mechanisms. The bacterial cell membrane will ultimately rupture, destroying the bacteria [6,7].

*Corresponding author
Email: seifoddini@yazd.ac.ir
Address: Department of Mining and Metallurgical Engineering, Yazd University, Yazd, Iran
1. Ph.D. Candidate, 2. Associate Professor, 3. Associate Professor, 4. Assistant Professor

DOI: http://10.22034/IJISSI.2024.2037010.1299
Published by ISSI (Iron & Steel Society of Iran)

Surface roughness is another parameter that can affect the antibacterial behavior of the surface of a surgical instrument or the degree of bacterial adhesion to these instruments. This issue can be mitigated by applying Thin Film Metallic Glass (TFMG) materials, which have very smooth surfaces [8, 13-17]. Extensive studies have investigated the relationship between surface roughness and the adhesion of cancer cells. Studies show that the $Zr_{39}Cu_{39}Ag_{22}$ TFMG [18], Zr-Cu-Al-Ag TFMG [19], $Zr_{46}Ti_{40}Ag_{14}$, and $Zr_{46}Ti_{43}Al_{11}$ Zr-based TFMGs [20] can reduce the adhesion of two common hospital bacteria resistant to penicillin, Escherichia coli and Staphylococcus aureus, or hinder their growth, multiplication, and movement.

The corrosion behavior of these coatings in different environments has also been extensively studied. The results indicate an increase in the corrosion resistance of these amorphous coatings compared to various uncoated substrates[21-26]. Investigations into the corrosion behavior of $Zr_{55}Al_{10}Ni_5Cu_{30}$ TFMG [21], Zr-Cu-Ni-Al, Zr-Ti-B-Si TFMG with different percentages of silicon, and $Zr_{48}Cu_{36}Al_8Ag_8$ TFMG [24,25] indicate that applying these coatings increases corrosion resistance compared to the substrate.

Hydrophilicity or hydrophobicity of a surface can also indicate its corrosion resistance. Studies show that Zr-based amorphous coatings are more corrosion-resistant than the substrate due to their high hydrophobicity (or reducing the contact angle) [27-31].

Another feature of Zr-based TFMG is their low surface free energy, which increases the corrosion resistance of these coatings. Summarized results about a wide range of TFMG coatings show that lower surface energy results in higher corrosion resistance [32, 20].

Therefore, it seems that applying a thin layer of designed Zr-based TFMG with a chemical composition of $Zr_{30}Cu_{20}Al_{10}Ag_{10}Cr_{10}Si_{10}B_{10}$ due to its amorphous structure, high surface smoothness, and good adhesion to the substrate can increase the corrosion resistance of the 316 stainless steel substrate.

2. Materials and Experimental Procedure

2.1. Materials

This research used metal powders with a high degree of purity to prepare the alloy and make the sputtering coating target. These materials include zirconium, silicon, aluminum, chromium, boron, copper, and silver powders. Additionally, argon gas, stearic acid, 316L stainless steel, silicon wafers (as substrates), and metallography materials were used. The chemical composition of 316 stainless steel used is given in Table 1.

The amount of powders used to fabricate the $Zr_{30}Cu_{20}Al_{10}Ag_{10}Cr_{10}Si_{10}B_{10}$ alloy is presented in Table 2.

2.2. Experimental Procedure

First, the raw material powders were weighed according to stoichiometric ratios. A digital scale with an accuracy of 0.001 grams was used. After adding half a gram of stearic acid to the powders, they were homogenized using a PM100 model ball mill in an argon atmosphere.

After mixing the powders, a Spark Plasma Sintering (SPS) system was used to prepare the target needed for sputtering. The sintering operation was conducted at a temperature of 850°C, a pressure of 40 MPa, a current of 1100 A, and a voltage of 2.5 W for 10 minutes. The mixed powder was poured into a graphite mold with a diameter of 50.8 mm and then subjected to sintering.

2.2.1. Deposition by DC Magneton Sputtering System

The deposition was performed on 316 stainless steel samples and p-type Si (100) wafers with dimensions of 1x1 cm. The samples were coated using a three-cathode DC Magnetron Sputtering device equipped with a turbomolecular pump capable of reaching a final vacuum of 8×10^{-6} torr. The sputtering was done at a working pressure of 8.9×10^{-3} torr, a power of 104 W, a current of 0.3 A, and a deposition time of 60 minutes.

Table 1. Chemical composition of 316 stainless steel used (Wt%).

C	Ni	Cr	Mo	Mn	Si	N	P	S	Fe
0.023	**11.280**	**17.024**	**2.231**	**1.191**	**0.582**	**0.045**	**0.028**	**0.006**	**Rem.**

Table 2. The number of primary powders used for fabrication of the alloy.

Element	Zr	Cu	Al	Ag	Cr	Si	B
at%	**30**	**20**	**10**	**10**	**10**	**10**	**10**
wt%	**43.7**	**20.3**	**4.3**	**17.2**	**8.3**	**4.5**	**1.7**

2.2.2. Structural studies

Scanning Electron Microscopy (SEM), Field Emission Scanning Electron Microscope (FESEM), and Atomic Force Microscope (AFM) were used to study the microstructure of the fabricated target, the surface morphology, and the thickness of the coated layers. X-ray diffraction (XRD) equipped with Incident Beam Grazing (GIXRD) was used to analyze the produced thin layer and ensure the amorphousness of the coating structure.

2.2.3. Measuring the Hydrophobicity of the Coatings

A CA-500A model contact angle measurement system, equipped with a camera and software for measuring the contact angle of a drop on a solid surface, was used to measure the hydrophobicity of the samples and determine the contact angle.

2.2.4. Investigating the Corrosion Behavior of coatings

Electrochemical potentiodynamic polarization tests were used to investigate the corrosion behavior of the prepared thin films. These tests were conducted using an IVIUM model potentiostat/galvanostat device and in a 3.5 wt% NaCl aqueous solution at ambient temperature.

2.2.5. Examining the Antibacterial Behavior of Coatings

The antibacterial behavior of the coating against two bacteria, Staphylococcus aureus (ATCC 25923) and Escherichia coli (ATCC 25922), were evaluated according to standard number Z2801:2000. After performing this test, the number of remaining live bacteria on each sample was counted, and the antibacterial rate of 316 stainless steel and the thin layer coating was calculated. The examination time was 24 hours.

3. Results and Discussion

3.1. Structural Studies of the Fabricated Target

The structural study of the fabricated target using the SPS method and the distribution of different elements in the target were performed using the FESEM microscope. As shown in Fig. 1. all elements are uniform in the fabricated target.

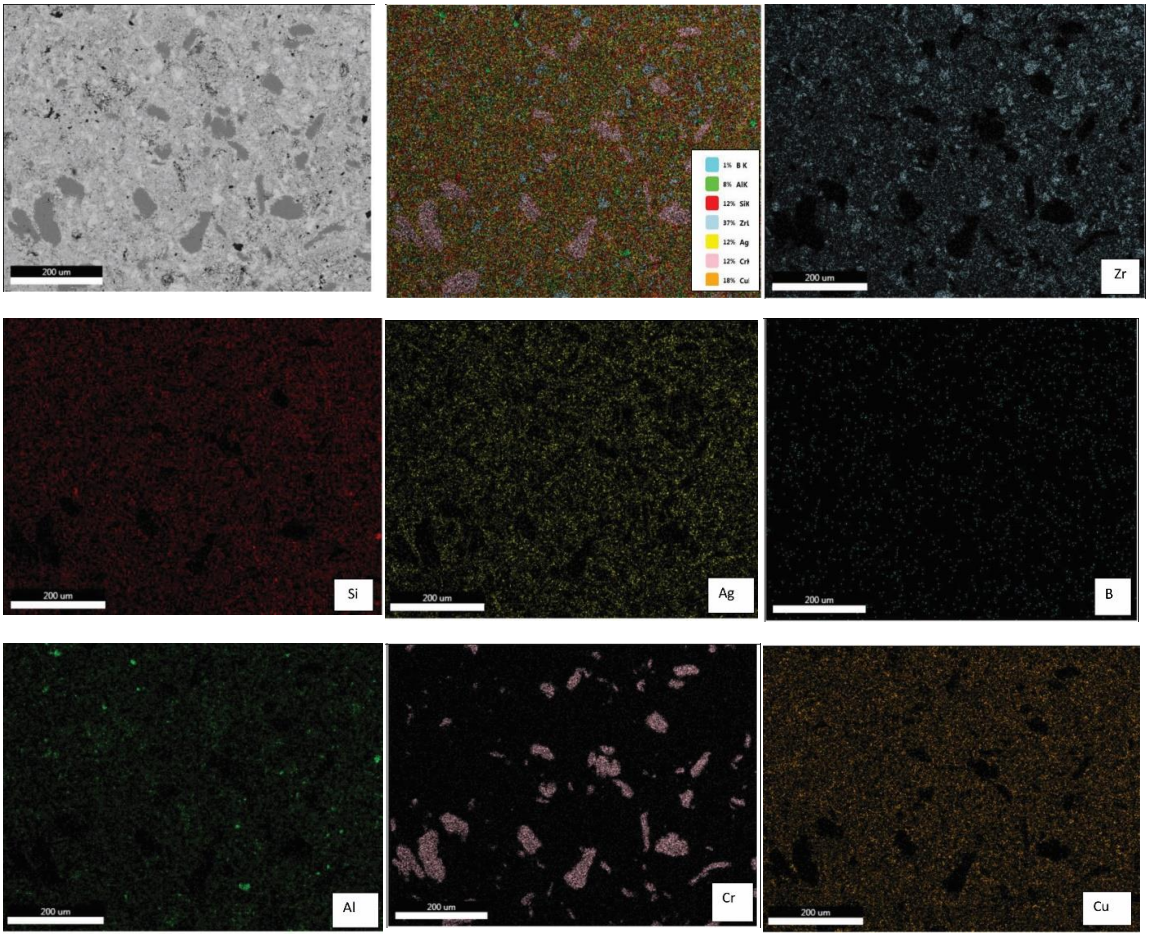

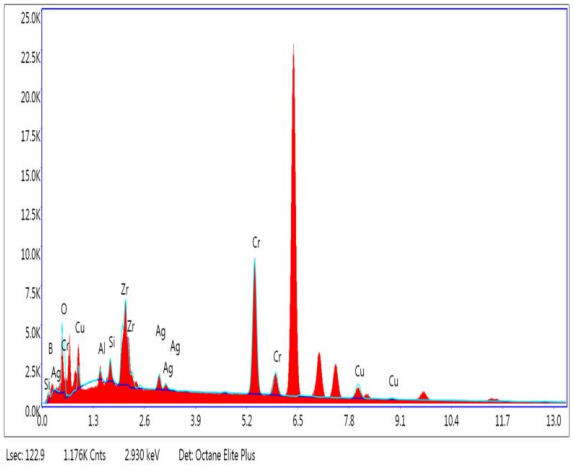

Element	Weight %	Atomic %
B K	18.12	50.99
O K	3.64	6.93
AlK	1.27	1.44
SiK	2.09	2.26
ZrL	11.38	3.80
AgL	4.23	1.19
CrK	47.30	27.67
CuK	11.96	5.73

Fig. 1. Elemental map and EDAX chemical analysis of the target fabricated by the SPS method.

3.2. Characterization of Coatings

The X-ray diffraction test at a very low angle, GIXRD, was used to ensure the amorphousness of the thin films that were produced. Fig. 2. shows the grazing X-ray diffraction pattern of the coating with the composition $Zr_{30}Cu_{20}Al_{10}Ag_{10}Cr_{10}Si_{10}B_{10}$. The absence of specific peaks in this graph indicates the absence of any crystal structure in the sample. Therefore, with more certainty, it can be said that the coating has an amorphous structure. Before doing any experiment, an amorphous structure can be predicted due to the very low thickness of the coating and the high rate of solidification.

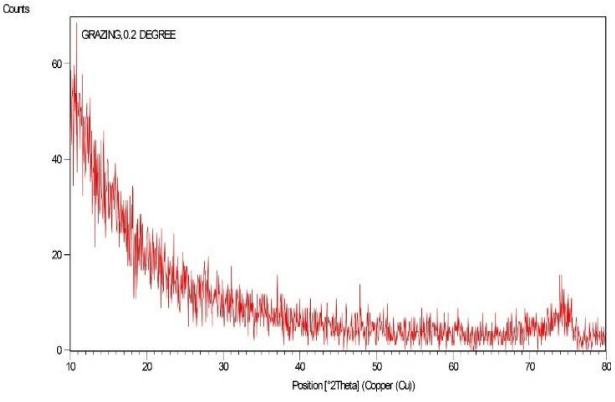

Fig. 2. GIXRD pattern of the thin layer produced with a power of 104 W, (0.3 A).

Fig. 3. shows the microscopic image of the cross-section of the created coating. Measuring the thickness of the coatings using the FESEM microscope showed that this coating has a thickness of 1.10 microns. As can be seen, the coating has relatively good surface smoothness and uniform thickness. Additionally, there is very good adhesion at the interface between the coating and the substrate.

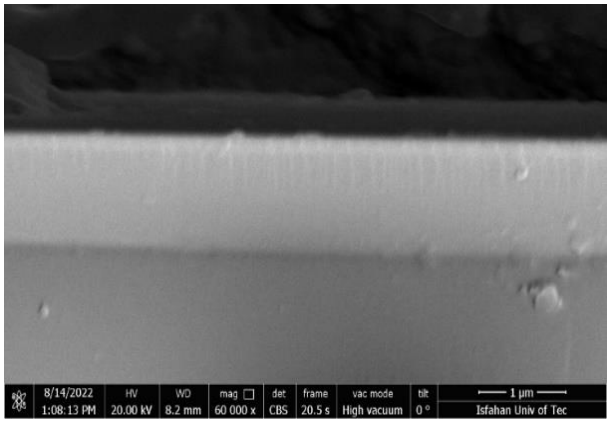

Fig. 3. Microscopic image of the cross-section of the produced TFMG coating.

Fig. 4. shows the elemental map related to the distribution of different elements in the coating on the entire sample surface. It can be seen that the distribution of these elements is completely uniform.

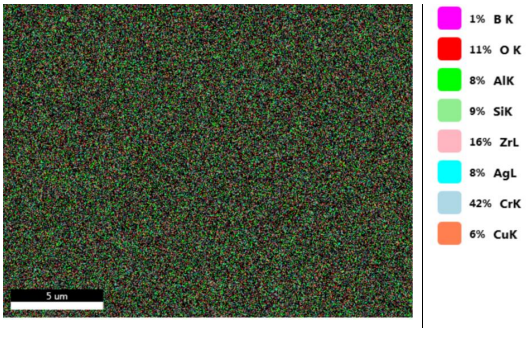

Fig. 4. X-ray map of the distribution of the elements in the TFMG coating.

Fig. 5. shows the FESEM image of the cross-section of the coating along with the EDAX chemical analysis of the coating. The pattern shows that all the elements used in the target are also present in the coating.

The examination carried out by the FESEM microscope also shows that the TFMG coating has a columnar structure, as seen in Fig. 6. The presence of a columnar structure in TFMG coatings has been reported by other researchers [33, 34]. It should be noted that despite a columnar structure, the coating seems to have good surface smoothness.

3.3. Antibacterial Behavior of the Coating

As mentioned, two of the most problematic bacteria that can cause infection are Staphylococcus Aureus and Escherichia Coli. These antibiotic-resistant bacteria have caused severe problems worldwide in recent years. Therefore, in this research, the antibacterial behavior of a novel Zr-based TFMG coating with the composition $Zr_{30}Cu_{20}Al_{10}Ag_{10}Cr_{10}Si_{10}B_{10}$ against these two bacteria was studied based on standard number Z2801: 2000 [35].

3.3.1. The Rate of Antibacterial

According to the mentioned standard, after exposing 316 stainless steel samples and the coated samples to the two bacteria, keeping them in a vibrating incubator for a certain period, performing dilution operations in 5 stages, culturing the remaining live bacteria in Mueller-Hinton

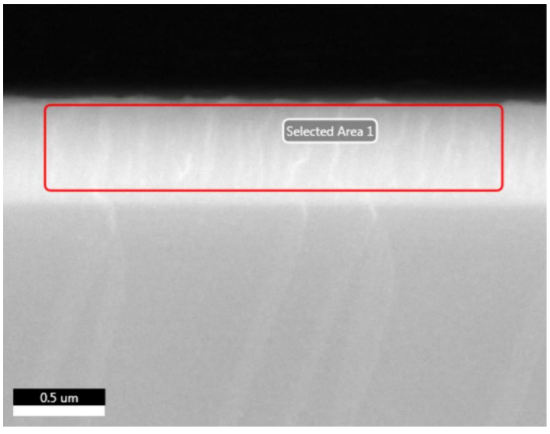

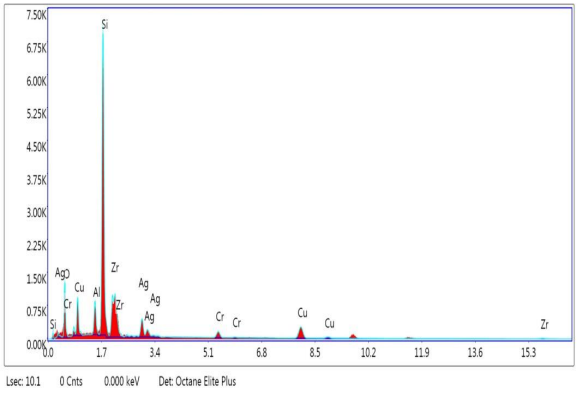

Element	Weight %	Atomic %
O K	19.73	37.72
AlK	4.76	5.40
SiK	39.76	43.31
ZrL	15.44	5.18
AgL	8.40	2.38
CrK	2.56	1.50
CuK	9.35	4.50

Fig. 5. Microscopic image of the cross-section of the coating along with the EDAX chemical analysis of the coating.

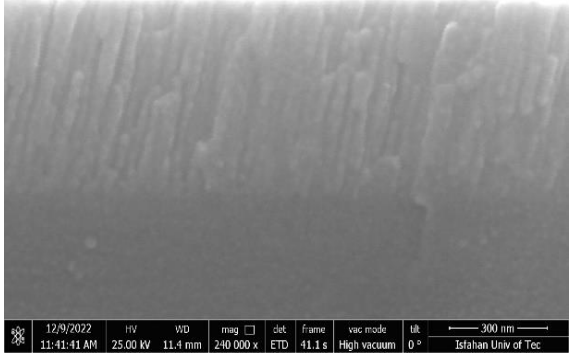

Fig. 6. The presence of a columnar structure in TFMG coating.

medium, and finally taking pictures and counting them, the antibacterial rate of the coatings against these two bacteria was calculated using Eq.(1)[31].

$$\text{Rate of Antibacterial } \% = \frac{N0 - N}{N0} \times 100 \quad \text{Eq.(1)}$$

Meanwhile, N_θ and N are the number of live bacteria remaining on the surface of the uncoated sample and the coated sample, respectively.

In Figs. 7. a and b. images of Staphylococcus aureus and Escherichia coli bacteria present on the 316 stainless steel sample at the initial moments of contact with the substrate and before any dilution operation are shown. As mentioned earlier, the initial concentration of bacteria is around 10^6 bacteria/ml.

In Figs. 8. a and b. images of live Staphylococcus aureus and Escherichia coli bacteria present on the 316 stainless steel sample at the end of the test and after five dilution stages are shown. The large number of living bacteria remaining on the substrate indicates the lack of any antibacterial properties of 316 stainless steel. The number of Staphylococcus aureus bacteria remaining on the 316 stainless steel substrate after the final dilution is 1110 CFU/ml, and for Escherichia coli, it is 1220 CFU/ml.

Picturing and counting the remaining live bacteria on the TFMG samples show that the number of live Staphylococcus aureus bacteria remaining on the coating is 23 CFU/ml. Additionally, the number of live Escherichia coli bacteria remaining on the coating is 32 CFU/ml. Figs. 9. a and b. show images of live Staphylococcus aureus and Escherichia coli bacteria remaining on the TFMG samples at the end of the test and after five dilution steps.

Using the initial number of bacteria and the number of remaining live bacteria on the TFMG coating and applying the given equation, the antibacterial rate of the coating can be calculated. The results show that the antibacterial rates of the coating were 98% and 97% for Staphylococcus aureus and Escherichia coli, respectively. It seems that no significant difference exists in the antibacterial behavior of the coating against these two bacteria. The high percentages of copper, silver, and aluminum elements in the coating contribute to its excellent antibacterial behavior. Similar results have been reported for other TFMG coatings containing these elements [18-20, 25-26]. The main reason for the antibacterial effect of the produced coating is the presence of silver and copper elements in the coating. The ions of these two elements destroy the cell membrane and easily enter the cell. They attach to the membrane proteins and disrupt their function, resulting in bacterial death due to lack of nutrition.

3.4. Roughness of Coatings and Adhesion of Cancer Cells to Them

The degree of adhesion of cancer cells to surgical instruments is considered one of the most up-to-date challenges in medical engineering. Surgical instruments used to remove a cancerous tumor allow cancer cells to adhere to them when they come into direct contact with the tumor tissue. Once attached to these tools, these cancer cells are often alive and transferred to healthy tissues, potentially giving rise to new cancerous tumors. Therefore, finding solutions to reduce the number of cells sticking to surgical instruments is one of the current challenges in medical engineering.

Considering the importance of the surface roughness of a medical instrument in the adhesion of cancer cells and platelets, the surface roughness of fully polished 316 stainless steel and $Zr_{30}Cu_{20}Al_{10}Ag_{10}Cr_{10}Si_{10}B_{10}$ alloy coating applied to this steel were compared and evaluated. Figs. 10 and 11. show the roughness curves and images obtained from the surfaces of these samples by AFM microscope.

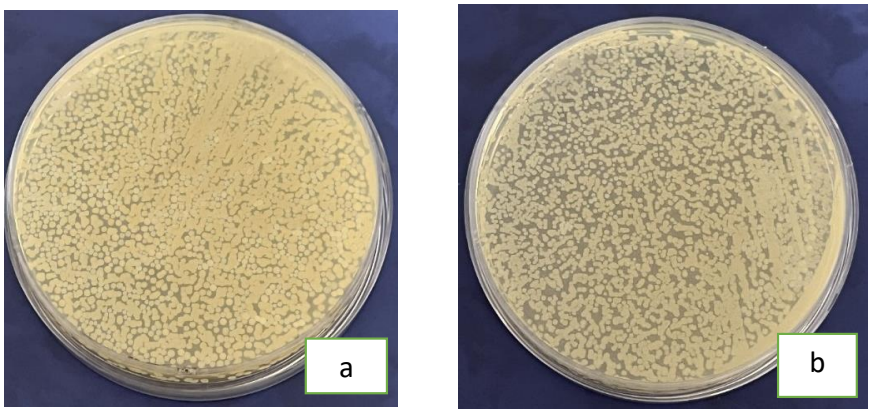

Fig. 7. Pictures of the two bacteria: a) Staphylococcus aureus and b) Escherichia coli present on the 316 stainless steel sample at the initial moments of contact and before any dilution operation.

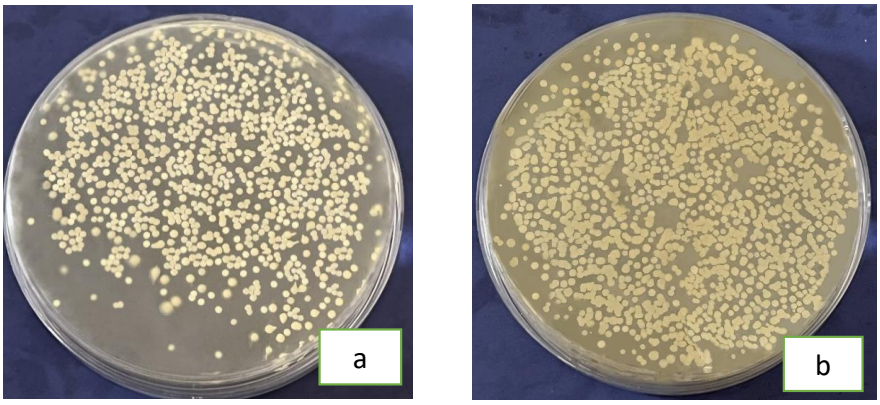

Fig. 8. Pictures of remaining living bacteria: a) Staphylococcus aureus and b) Escherichia coli on the 316 stainless steel sample at the end of the test and after five stages of dilution.

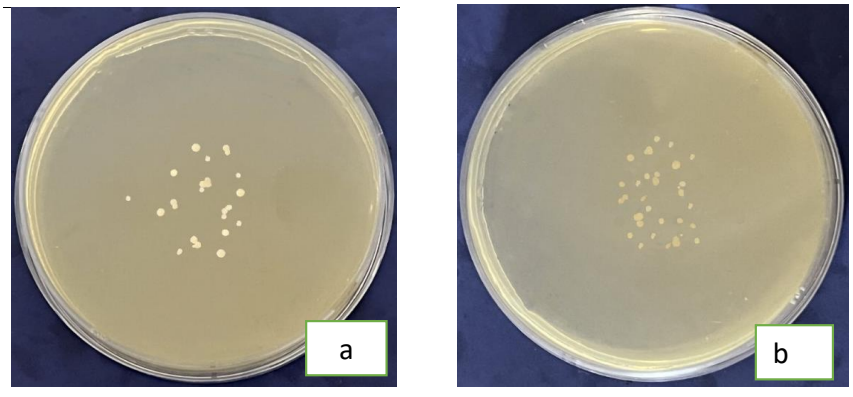

Fig. 9. Images of the remaining live bacteria a) Staphylococcus aureus and b) Escherichia coli on the TFMG samples at the end of the test and after five dilution steps.

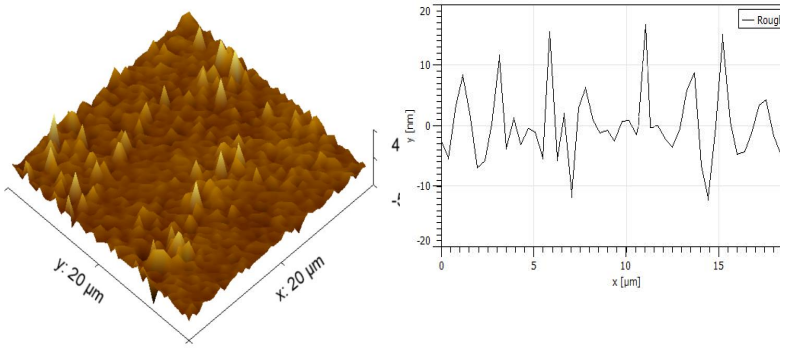

Fig. 10. Roughness curves and 3D image of as-polished 316 stainless.

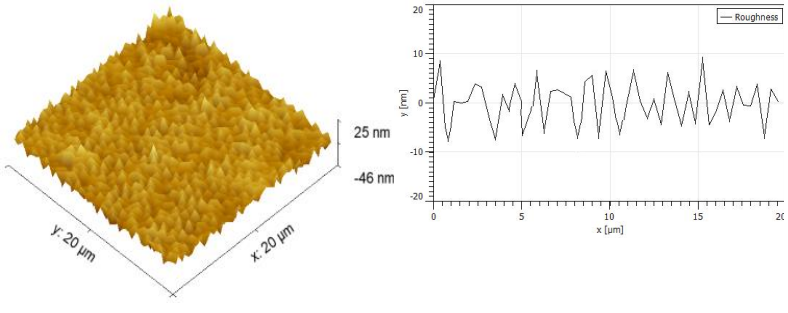

Fig. 11. Roughness curve and 3D image of TFMG coating applied on 316 stainless steel.

The results indicate that the surface roughness of the 316 stainless steel substrate in the fully polished state equals Ra = 8.08 nm, and for the TFMG-coated sample, it equals Ra = 2.11 nm. This shows that applying the coating has increased the smoothness of the substrate by 48%.

Therefore, if this TFMG coating is applied to medical instruments made of 316 stainless steel, it can play an essential role in preventing post-surgical infections. Observations by others also confirm the existence of a direct relationship between the adhesion level of various human and animal platelet cells and cancer cells and the surface roughness of surgical tools [15, 36-43].

3.5. Hydrophobicity of the Coatings

The degree of hydrophobicity of a surface can significantly impact corrosion rates and even the adhesion of bacteria to that surface. Therefore, a hydrophobic coating must be applied to medical and hospital instruments.

Surfaces can be classified according to their contact angle with water. Those with an angle close to zero are considered superhydrophilic; less than 90 degrees are hydrophilic, between 90 and 150 degrees are hydrophobic, and more than 150 degrees are superhydrophobic. These classifications are illustrated in Figs 12 and 13. which show the wettability of uncoated and coated 316 stainless steel substrates, respectively.

The contact angle for polished stainless steel 316 is 75±1 degrees, and for the TFMG coating, it is 106±3 degrees. Applying the TFMG coating increases the contact angle, improving the hydrophobicity of the substrate.

Based on the above classification, the 316 stainless steel surface is hydrophilic, and the $Zr_{30}Cu_{20}Al_{10}Ag_{10}Cr_{10}Si_{10}B_{10}$ TFMG coating is hydrophobic. The hydrophobicity of the coating is due to its smoother surface and amorphous structure compared to the substrate.

Consequently, higher corrosion resistance and better antibacterial behavior are expected for the coated samples. Other researchers have also shown that applying a TFMG layer on different substrates increases the contact angle and hydrophobic properties [26, 29-31].

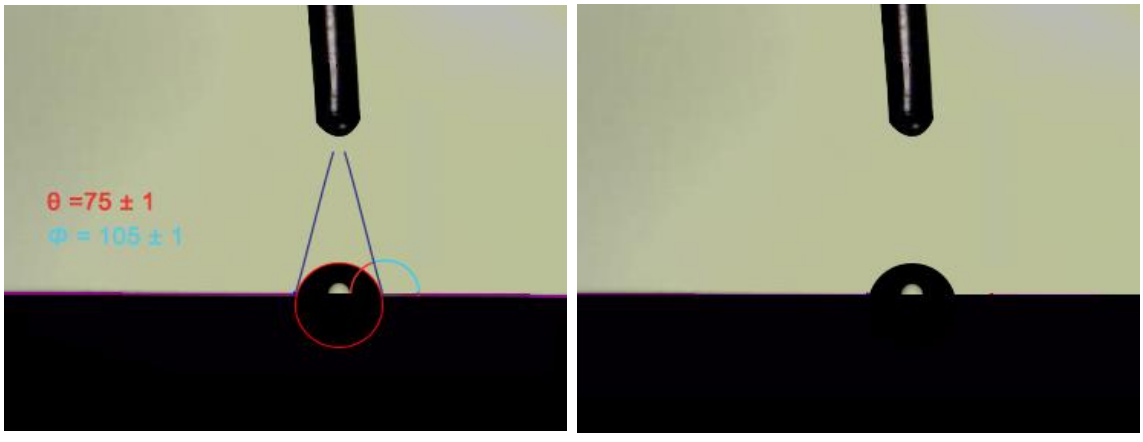

Fig. 12. Wettability test of 316 stainless steel without coating, (contact angle: 75 ± 1 degree).

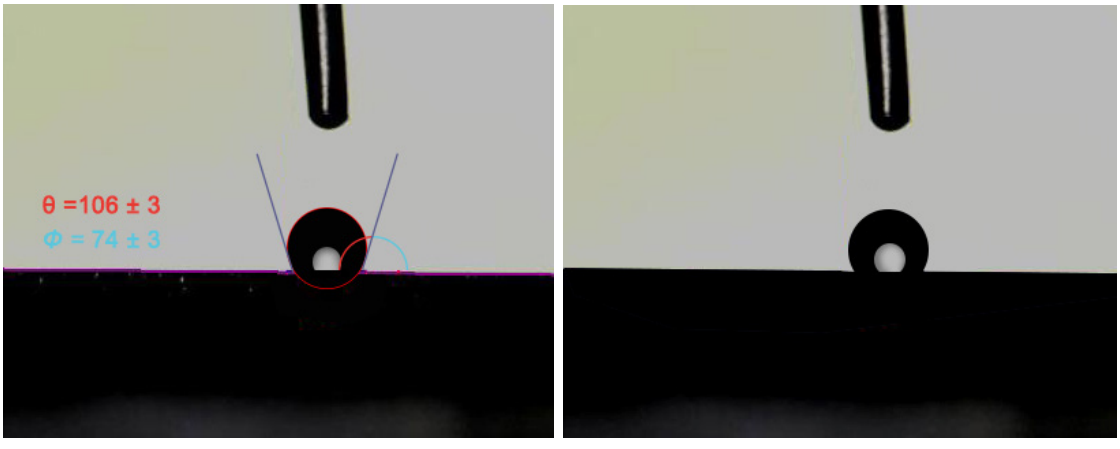

Fig. 13. Wettability test of the coating with a thickness of 1.1 microns (contact angle:106±3 degrees).

3.6. Wettability and Surface Energy of the Coatings

One of the most critical factors affecting the contact angle is the surface energy on which the liquid phase is placed. Coatings with lower surface free energy can reduce the corrosion rate of the surface.

As shown in Table 3. the reduction of surface energy increases the contact angle, enhancing the hydrophobic properties of the surfaces. The surface energy of the 316 stainless steel substrate is 91.6 mJ/m², while for the TFMG coating, it is 52.7 mJ/m²: a reduction of 42%. This reduction significantly improves the stainless steel substrate's corrosion behavior and antibacterial properties.

The surface energy of the 316 stainless steel substrate and the coating is calculated using the following equation, Eq.(2) [45]:

$$\text{Surface Energy} = \gamma \times (1 + \cos\theta) \qquad \text{Eq.(2)}$$

Where θ is the contact angle and γ is the surface energy of the liquid drop in contact with the surface. The surface energy of the water is equal to 72.8 mJ/m² [45].

Previous findings also show that lower surface energy leads to a lower contact angle, reducing the adhesion tendency of materials to the surface [17, 20].

3.7. Corrosion of the TFMG Coatings

Before conducting the corrosion tests, it is expected that applying the Zr-based TFMG coating on the 316 stainless steel substrate will increase the corrosion resistance of the substrate due to the coating's hydrophobicity.

The electrochemical potentiodynamic polarization test is used to study the corrosion behavior of a coating. In this test, the corrosion potential parameter (E_{corr}) evaluates the corrosion driving force, and the corrosion current parameter (I_{corr}) evaluates the corrosion current intensity. In this research, the corrosion behavior of 316 stainless steel samples before and after coating was compared by potentiodynamic polarization tests in a 3.5% NaCl solution. Fig. 14. shows the potentiodynamic polarization curves of the 316 stainless steel substrate and the coated sample.

The results show that the corrosion potential of the coated sample is much higher than that of the 316 stainless steel substrate. In other words, thermodynamically, the possibility of corrosion is higher for the uncoated sample than for the coated sample. Based on the polarization tests in a 3.5% NaCl solution, the corrosion potential of stainless steel is -178 mV, and for the coating, it is 235 mV. The corrosion current density of the substrate is 46 nA/cm², while for the coating, it is 3.6 nA/cm². This result shows that the Z $Zr_{30}Cu_{20}Al_{10}Ag_{10}Cr_{10}Si_{10}B_{10}$ coating, due to its amorphous structure, hydrophobicity, and uniform chemical composition, has higher corrosion resistance than the 316 stainless steel substrate.

After the corrosion test, the surface morphology of the coated sample was analyzed using a scanning

Table 3. The contact angle and surface energy of the 316 stainless steel substrate and the TFMG coating.

Surface	Contact Angle (degree)	Surface Energy (mJ/m^2)
316 stainless steel	75±1	91.6
TFMG coating	106±3	52.7

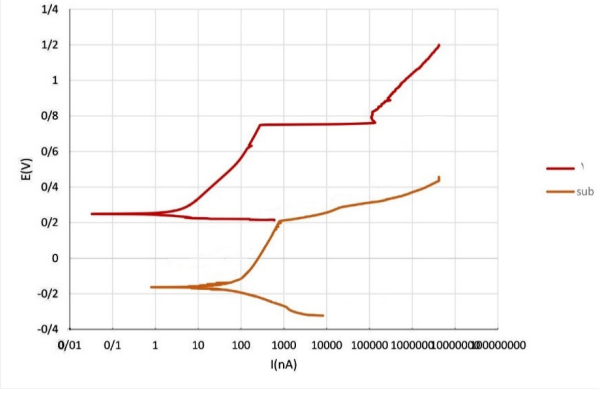

Fig. 14. Dynamic potential polarization curves of the 316 stainless steel substrate (curve 1) and Zr-based TFMG coating (curve 1) in a 3.5% NaCl solution.

electron microscope equipped with an EDS analysis system. Fig. 15. shows the SEM image of the coated sample surface after the corrosion test. The coating appears to remain primarily passive without any damage.

A limited number of holes can be observed on the surface at higher magnification. It seems that pitting corrosion has occurred. Fig. 16. shows the FESEM image of the sample surface along with the EDAX analysis of one of the holes.

A local analysis of one of the holes shows that the coating has completely disappeared in the hole area, and only the main elements of the stainless steel substrate are present in the analysis. Similar studies have confirmed the pitting corrosion phenomenon [31]. The obtained results have been confirmed by a large group of researchers [21-26].

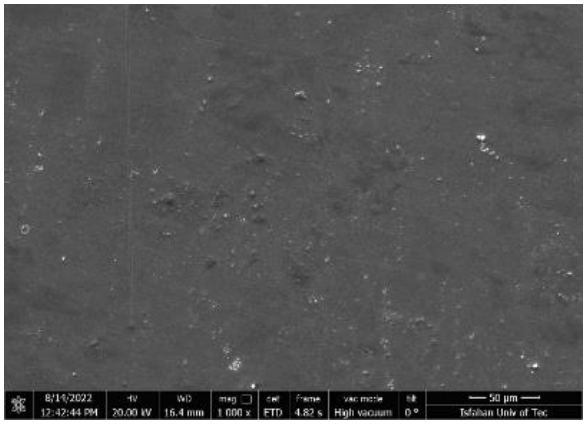

Fig. 15. SEM image of the coated sample surface after the corrosion test.

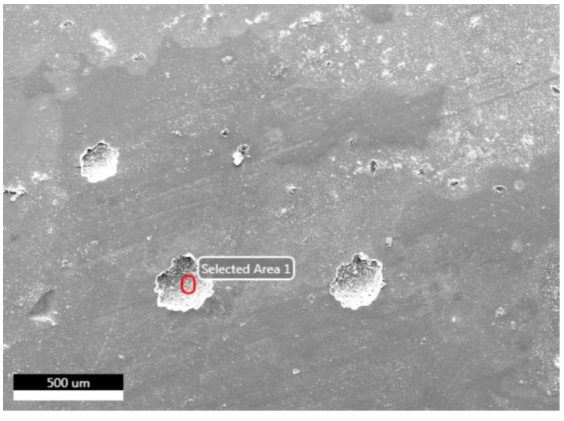

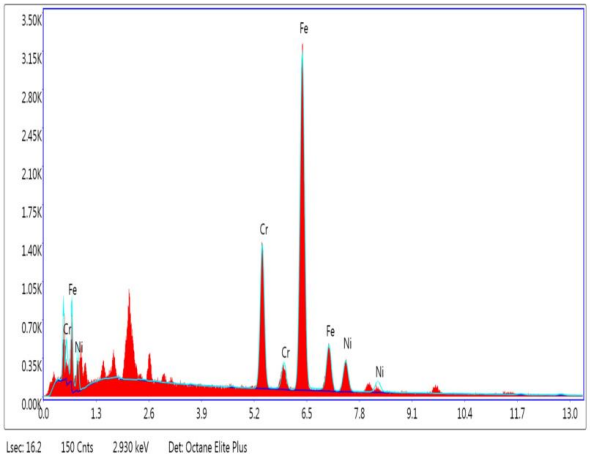

Element	Weight %	Atomic %
CrK	20.03	21.29
FeK	70.90	70.17
NiK	9.08	8.54

Fig. 16. Microscopic image of the coated sample surface after the corrosion test, along with the chemical analysis of one of the holes on the corroded surface.

4. Conclusions

- All elements have a uniform distribution in the fabricated target by the SPS method.
- The grazing X-ray diffraction pattern showed more certainty that the novel $Zr_{30}Cu_{20}Al_{10}Ag_{10}Cr_{10}Si_{10}B_{10}$ TFMG coating created on the 316 stainless steel substrate has an amorphous structure.
- The coating, with a columnar structure and 1.10 microns thickness, has excellent adhesion to the 316 stainless steel substrate.
- The newly designed coating showed good antibacterial behavior. The antibacterial rate of the coating was 98% and 97% for Staphylococcus aureus and Escherichia coli bacteria, respectively.
- Applying the designed coating has increased the smoothness of the polished 316 stainless steel substrate by 48%, which can diminish the adhesion level of various cancer cells to surgical tools fabricated from this steel.
- The coating can be applied by increasing the contact angle to transform the surface of 316 stainless steel from hydrophilic to hydrophobic.
- The coating has reduced the surface free energy by 42% of the polished 316 stainless steels. This factor can significantly improve this steel's corrosion behavior and antibacterial properties.
- The result showed that the $Zr_{30}Cu_{20}Al_{10}Ag_{10}Cr_{10}Si_{10}B_{10}$ coating, due to its amorphous structure and hydrophobicity, has a higher corrosion resistance compared to the 316 stainless steel substrate in a 3.5% NaCl solution.

References

[1] Hyde F.W, Alberg M, and Smith K, Comparison of fluorinated polymers against stainless steel, glass and polypropylene in microbial biofilm adherence and removal, Journal of Industrial Microbiology & Biotechnology. 1997, 19; :142–149.

[2] Rai M, Yadav A, and Gade A, Silver nanoparticles as a new generation of antimicrobials, Biotechnology Advances. 2009; 27: 76–83.

[3] Clement J.L, Jarrett P.S, Metal-Based Drugs, Antibacterial Silver. 1994; 1: 467-482.

[4] Borkow G and Gabbay J, Copper, An Ancient Remedy Returning to Fight Microbial, Fungal and Viral Infections, Current Chemical Biology. 2009; 3: 272-278.

[5] Borkow G and Gabbay J, Copper as a Biocidal Tool, Current Medicinal Chemistry. 2005; 12: 2163-2175.

[6] Grass G, Rensing C, and Solioz M, Metallic Copper as an Antimicrobial Surface, Applied and Environmental Microbiology. 2011; 75: 1541–1547.

[7] Dallas P, Sharma V.K, Zboril R, Silver polymeric nanocomposites as advanced antimicrobial agents: Classification, synthetic paths, applications, and perspectives, Advances in Colloid and Interface Science. 2011; 1662: 119-135.

[8] Chu J.P, Liu T.Y, Li C. L, Wang C.H, Jang J.S.C, Chen M.J, Chang S.H, Huang W.C, Fabrication and characterizations of thin film metallic glasses: antibacterial property and durability study for medical application, Thin Solid Films 561. 2014: 102–107.

[9] Truong V.K, Lapovok R, Estrin Y.S, Rundell S, Wang J.Y, Fluke C.J, Crawford R.J, Ivanova E.P, The influence of nano-scale surface roughness on bacterial adhesion to ultrafine-grained titanium, Biomaterials. 2010; 31: 3674–3683.

[10] Wang Y.B, Li H.F, Cheng Y, Zheng Y.F, Ruan L.Q, In vitro and in vivo studies on Ti-based bulk metallic glass as potential dental implant material, Mater. Sci. Eng. 2013; 33: 3489–3497.

[11] Schroers J, Kumar G, Hodges T.M, Chan S, Kyriakides T.R, Bulk metallic glasses for biomedical applications, JOM 2009; 61: 21–29.

[12] Howlett C.R, Evans M.D.M, Walsh W.R, Johnson G, Steele J.G, Mechanism of initial attachment of cells derived from human bone to commonly used prosthetic materials during cell culture, Biomaterials. 1994; 15: 213–222.

[13] Hallab N.J, Bundy K.J, O'Connor K, Moses R.L, Jacobs J.J, Evaluation of metallic and polymeric biomaterial surface energy and surface roughness characteristics for directed cell adhesion, Tissue Eng. 7 roughness characteristics for directed cell adhesion, Tissue Eng. 2001; 7: 55–71.

[14] Lampin M, Warocquier-Clérout R, Legris C, Degrange M, Sigot-Luizard M.F, Correlation between substratum roughness and wettability, cell adhesion, and cell migration, J. Biomed. Mater. Res. 1997; 36: 99–108.

[15] Deligianni D.D, Katsala N.D, Koutsoukos P.G, Missirlis Y.F, Effect of surface roughness of hydroxyapatite on human bone marrow cell adhesion, proliferation, differentiation and detachment strength, Biomaterials. 2001; 22: 87–96.

[16] Bourassa M.G, Cantin M, Sandborn E.B, Pederson E, Scanning electron microscopy of surface irregularities and thrombogenesis of polyurethane and poly-ethylene coronary catheters, Circulation. 1976; 53: 992–996.

[17] Huang Q, Yang Y, Hu R, Lin C, Sun L, Vogler E.A, Reduced platelet adhesion and improved corrosion resistance of superhydrophobic TiO_2-nanotube-coated 316L stainless steel, Colloids Surf. B: Biointerfaces. 2015; 125: 134–141.

[18] Etiemble A, Der Loughian C, Apreutesei M, Langlois C, Cardinal S, Pelletier J.M, Pierson J.P, Steyer P, Innovative Zr-Cu-Ag thin film metallic glass deposed by magnetron PVD sputtering for antibacterial applications, Journal of Alloys and Compounds. 2017; 707:155-161.

[19] Chen H.W, Hsu K, Chan Y.Ch, Duh J.G, Lee J.W, Shian-Ching Jang J, Chen G.J., Antimicrobial properties of Zr–Cu–Al–Ag thin film metallic glass, Thin Solid Films. 214; 561: 98–101.

[20] Jabed A, Mudasser Khan M, Camiller J, Greenlee-Wacker M, Shabib I, Property optimization of Zr-

Ti-X (X = Ag, Al) metallic glass via combinatorial development aimed at prospective biomedical application, Surface and Coatings Technology. 2019; 37225: 278-287.
[21] Qin F.X, Wang X.M, Xie G.Q, Microstructure and electrochemical behavior of Ti-coated $Zr_{55}Al_{10}Ni_5Cu_{30}$ bulk metallic glass, Intermetallics. 2009; 17: 945–950.
[22] Chuang C.Y, Liao Y.C, Lee J.W, Li C.L, Duh J.G, Electrochemical characterization of Zr-based thin film metallic glass in hydrochloric aqueous solution, Thin Solid Films. 2013; 5291: 338-341.
[23] Deng Y. L, Lee J.W, The fabrication and property evaluation of Zr–Ti–B–Si thin film metallic glass materials, Surface and Coatings Technology. 2014; 259 :115-122.
[24] Rajan S.T, Karthika M, Bendavid A, Subramanian B, Apatite layer growth on glassy $Zr_{48}Cu_{36}Al_8Ag_8$ sputtered titanium for potential biomedical applications, Applied Surface Science. (2016); 369: 501-509.
[25] Subramanian B, Yugeswaran S, Kobayashi A, Jayachandran M, Fabrication of amorphous $Zr_{48}Cu_{36}Al_8Ag_8$ thin films by ion beam sputtering and their corrosion behavior in sbf for bio implants, Journal of Alloys and Compounds. 2013; 572: 163-169.
[26] Subramanian B, In vitro corrosion and biocompatibility screening of Sputtered $Ti_{40}Cu_{36}Pd_{14}Zr_{10}$ thin film metallic glasses on steels, Materials Science and Engineering C. 2015; 47: 48–56.
[27] Ishizaki T, Saito N, Rapid formation of a superhydrophobic surface on a magnesium alloy coated with a cerium oxide film by a simple immersion process at room temperature and its chemical stability, Langmuir. 2010; 26: 9749-9755.
[28] BarKhudarov P.M, Shah P.B, Watkins E.B, Doshi D.A, Brinker C. J, Majewski J, Corrosion inhibition using superhydrophobic films, Corrosion Science. 2008; 50: 897-902.
[29] Yoldi M, Garcia J, Rodriguez R, Fabrication of superhydrophobic nanostructured films by physical vapour deposition, Nanotech. 2010; 1: 600-603.
[30] Chu J.H, Lee J, Chang C.C, Chan Y.C, Liou M.L, Lee J.W, Jang J.S.C, Duh J.G., Antimicrobial characteristics in Cu-containing Zr-based thin film metallic glass, Surface & Coatings Technology. 2014; 259: 87-93.
[31] Lee J, Liou M.L, Duh J.G, The development of a Zr-Cu-Al-Ag-N thin film metallic glass coating in pursuit of improved mechanical, corrosion, and antimicrobial property for bio-medical application , Surface and Coatings Technology. 2017; 310: 214-222.
[32] Yiu P, Diyatmika W, Bönninghoff N, Lu Y.C, Lai B.Z, Chu J.P, Thin film metallic glasses: Properties, applications and future, Journal of Applied Physic. 2020; 127: 1-16.
[33] Chu J.H, Chen H.W, Chan Y.C, Duh J.G, Lee J.W, Jang J.S.C, Modification of structure and property in Zr-based thin film metallic glass via processing temperature control, Thin Solid Films. 2014; 561: 38-42.
[34] Rauf A, Fang Y, Zhang H, Peng G, Feng T, Thickness effects on microstructure, mechanical and soft magnetic properties of sputtered Fe-Zr thin film metallic glass, Journal of Non-Crystalline Solids. 2019; 521: 119500.
[35] JIS Z2801, Antimicrobial Products test for Antimicrobial Activity and Efficacy, Japanese Industrial Standard. 2000: 2001.
[36] George J.N, Direct assessment of platelet adhesion to glass: a study of the forces of interaction and the effects of plasma and serum factors, platelet function, and modification of the glass surface, Blood. 1972; 40: 862–874.
[37] Vijayanad K, Pattanayak D.K, Mohan T.R, Banerjee R, Interpreting blood-bio-material interactions from surface free energy and work of adhesion, Trends Biomater. Artif. Organs. 2005; 18:73–83.
[38] Busch R, Strohbach A, Rethfeldt S, Walz S, Busch M, Petersen S, Felix S, Sternberg K, New stent surface materials: the impact of polymer-dependent inter-actions of human endothelial cells, smooth muscle cells, and platelets, Acta Biomater. 2014; 10: 688–700.
[39] May R.M, Magin C.M, Mann E.E, Drinker M.C, Fraser J.C, Siedlecki C.A, Brennan A.B, Reddy S.T, An engineered micropattern to reduce bacterial colonization, platelet adhesion and fibrin sheath formation for improved biocompatibility of central venous catheters, Clin. Transl. Med. 2015; 4: 9.
[40] Dowling D.P, Miller I.S, Ardhaoui M, Gallagher W.M, Effect of surface wettability and topography on the adhesion of osteosarcoma cells on plasma-modified poly-styrene, J. Biomater. Appl. 2011; 26: 327–347.
[41] Crear J, Kummer K.M, Webster T.J, Decreased cervical cancer cell adhesion on nanotubular titanium for the treatment of cervical cancer, Int. J. Nanomedicine 2013; 8: 995–1001.
[42] Chang C. H, Lib C. L, Yu C.C, Chen Y. L, Chyntara S, Ming-Jen Chen J. P. C, and Chang S.H, Beneficial effects of thin film metallic glass coating in reducing adhesion of platelet and cancer cells: Clinical testing, Surface & Coatings Technology. 2018; 344: 312–321.
[43] Furie B, Furie B.C, Mechanisms of thrombus formation, N. Engl. J. Med. 2008; 359: 938–94.
[44] Kota A.K, Kwon G, and Tuteja A, The design and applications of superomniphobic surfaces, NPG Asia Materials. 2014; 6: 1-16.
[45] Kaliaraj G.S, Ramadoss A, Sundaram M, Balasubramanian S, Muthirulandi J., Studies of calcium-precipitating oral bacterial adhesion on TiN, TiO_2 single layer, and TiN/TiO_2 multilayer-coated 316L SS, Journal of materials Science. 2014; 49: 7172–7180.